Interdiscip Toxicol. 2017; **Vol. 10**(4): 129–141.
doi: 10.1515/intox-2017-0019

DE GRUYTER OPEN

OPEN ACCESS

interdisciplinary toxicology

ORIGINAL ARTICLE

Oleuropein and rutin protect against 6-OHDA-induced neurotoxicity in PC12 cells through modulation of mitochondrial function and unfolded protein response

Zubeyir ELMAZOGLU [1], Volkan ERGIN [2], Ergin SAHIN [3], Handan KAYHAN [4], Cimen KARASU [1]

[1] *Department of Medical Pharmacology, Cellular Stress Response and Signal Transduction Research Laboratory, Gazi University, Faculty of Medicine, Ankara, Turkey*
[2] *Department of Medical Biology, Erzincan University, Faculty of Medicine, Erzincan, Turkey*
[3] *Department of Biology, Ankara University, Faculty of Science, Ankara, Turkey*
[4] *Department of Hematology, Gazi University, Faculty of Medicine, Ankara, Turkey*

ITX100417A01 • Received: 11 November 2017 • Accepted: 14 December 2017

ABSTRACT

Parkinson's disease (PD) is a highly prevalent neurodegenerative disorder, often associated with oxidative stress-induced transcriptional changes in dopaminergic neurons. Phenolic antioxidants, oleuropein (OLE) and rutin (RUT) have attracted a great interest due to their potential to counteract oxidative protein aggregation and toxicity. This study aimed at examining the effects of OLE and RUT against 6-OHDA-induced stress response in rat pheochromocytoma cells. When differentiated PC12 cells were exposed to oxidative stress composer 6-OHDA (100 µM, 8 h), a decreased mitochondrial membrane potential (ΔΨm) was observed along with a significant loss of cell viability and apoptotic nuclear changes. Exposure to 6-OHDA resulted in unfolded protein response (UPR) in differentiated PC12 cells as evidenced by an increased level of endoplasmic reticulum (ER)-localized transmembrane signal transducer IRE1α, adaptive response proteins ATF-4 and proapoptotic transcription factor CHOP. OLE or RUT pretreatment (24 h) at low doses (1–50 µM) protected the differentiated PC12 cells from 6-OHDA-induced cytotoxicity as assessed by increased viability, improved ΔΨm and inhibited apoptosis, whereas relatively high doses of OLE or RUT (>50 µM) inhibited cell growth and proliferation, indicating a typical hormetic effect. In hormetic doses, OLE and RUT up-regulated 6-OHDA-induced increase in IRE1α, ATF-4 and inhibited CHOP, PERK, BIP and PDI. 6-OHDA-activated XBP1 splicing was also inhibited by OLE or RUT. The presented results suggest that neuroprotection against 6-OHDA-induced oxidative toxicity may be attributable to neurohormetic effects of OLE or RUT at low doses through regulating mitochondrial functions, controlling persistent protein misfolding, activating and/or amplificating the adaptive response-related signaling pathways, leading to UPR prosurvival output.

KEY WORDS: oleuropein; rutin; neurotoxicity; mitochondria; endoplasmic reticulum

Introduction

Parkinson's disease (PD), the most common neurodegenerative movement disorder, is characterized by bradykinesia, muscular rigidity, and tremor. Both genetic and environmental factors play a crucial role in its pathogenesis (Fahn & Sulzer, 2004; Davie, 2008; Chao *et al.*, 2014). Although the molecular mechanisms remain to be fully elucidated, the pathogenesis of PD is generally recognized to be associated with impaired redox signaling, mitochondrial dysfunction, excitotoxicity, chronic inflammation, early apoptosis and synaptic loss in dopaminergic neurons (Ebrahimi-Fakhari *et al.*, 2012; Exner *et al.*, 2012).

Recent evidence emphasized that oxidative stress-mediated neuroinflammation is a key cellular component in the substantia nigra of patients with Parkinson's disease (Hauser & Hastings, 2013; Taylor *et al.*, 2013). A number of sources and mechanisms for the generation of reactive oxygen species (ROS) are recognized including the metabolism of dopamine itself, NADPH oxidases (NOX), Fenton reaction, neuroinflammatory cells, calcium, and aging (Taylor *et al.*, 2013; Dias *et al.*, 2013). Moreover, a growing body of evidence highlights an important role

Correspondence address:
Prof. Dr. Cimen Karasu
Cellular Stress Response and Signal Transduction Research Laboratory
Faculty of Medicine, Department of Medical Pharmacology
Gazi University, Besevler 06500, Ankara, Turkey.
TEL.: +90 312 2026921 • FAX +90 312 2124647
E-MAIL: cimenkrs@gmail.com

of mitochondrial dysfunction in PD since mitochondria contain many redox enzymes and naturally occurring inefficiencies of oxidative phosphorylation generate ROS in this organelle (Federico *et al.,* 2012; Taylor *et al.,* 2013; Dias *et al.,* 2013; Credle *et al.,* 2015). Thus considerable importance has been given to the prevention of oxidative stress as a potential therapeutic strategy. Most insights into the pathogenesis of PD come from experiments in nerve-growth-factor (NGF)-differentiated PC12 cells (neuronal PC12 cells) applied with neurotoxins such as 6-hydroxydopamine (6-OHDA). 6-OHDA is selectively taken up by catecholaminergic neurons and causes their damage or death by the combined effect of ROS and quinones (Meng *et al.,* 2007; Li *et al.,* 2014). 6-OHDA has also been demonstrated to cause mitochondrial damage, resulting over-production of ROS and DNA damage (Deng *et al.,* 2012; Kim *et al.,* 2012; Wang *et al.,* 2015).

Oxidative stress disrupts endoplasmic reticulum (ER) which is a key component of cellular protein homeostasis, controlling the regulation of protein trafficking, synthesis, folding, and degradation (Perri *et al.,* 2016). The implementing process in protein quality control in the ER is the unfolded protein response (UPR), which is activated upon ER stress to reestablish homeostasis through a sophisticated transcriptionally and translationally regulated signaling network (Hoozemans & Scheper, 2012; Cai *et al.,* 2016). Accumulation of misfolded proteins within the ER activates the UPR resulting in the execution of adaptive or non-adaptive signaling pathways. It is well established that aggregation and accumulation of misfolded proteins is responsible for neurodegeneration in PD (Benyair *et al.,* 2011).

The current therapeutic strategies available for PD temporarily ameliorate some of the clinical symptoms but do not stop or slow down the underlying degenerative processes. Recently, enormous efforts have been deployed to formulate new strategies that address neuronal degeneration. The latest studies indicated that mitochondrial dysfunction and ER-stress targeted regimens could be a potential approach to overcome neurodegeneration (Kondratyev *et al.,* 2007; Benyair *et al.,* 2011; Hoozemans & Scheper, 2012; Leitman *et al.,* 2013; Cai *et al.,* 2016; Ogen-Shtern *et al.,* 2016). Following this line of evidence, a few recent studies showed that some natural polyphenolic compounds exhibited neuroprotective effects by regulation of redox stress-mediated UPR response (Wu *et al.,* 2015; Cheng *et al.,* 2016). Natural polyphenols exert their beneficial effects also by different means including the modulation of key steps in redox signaling pathways, limitation of neuroinflammation, inhibition of apoptosis and activation of autophagy (El-Horany *et al.,* 2016; Ataie *et al.,* 2016).

Of them, oleuropein (OLE) is a polyphenolic compound, derived from *Olea europea,* reported to exert numerous pharmacological benefits including, anti-oxidative, anti-inflammatory, anti-atherogenic, antitumor, hypoglycemic, hepatoprotective, and neuroprotective activities (Rigacci & Stefani, 2016). We demonstrated that OLE protected the cells against cytokine-induced damage (Cumaoglu *et al.,* 2011a, 2011b) and 4-hydroxynonenal-induced toxicity through maintenance of redox homeostasis (Bali *et al.,* 2014). Its effectiveness also against Alzheimer's disease has recently been emphasized (Casamenti *et al.,* 2015; Martorell *et al.,* 2016). OLE is reported to improve learning and memory retention, and to attenuate cognitive dysfunction in a rat model of oxidative damage (Pourkhodadad *et al.,* 2016; Alirezaei *et al.,* 2016; Pantano *et al.,* 2017). OLE also reduces the oxidative damage in midbrain and dopaminergic neurons of substantia nigra by increasing the antioxidant enzyme activities in old rats (Sarbishegi *et al.,* 2014). Recent studies showed protective effects of OLE against 6-OHDA-induced degeneration and apoptosis via mitigating mitochondrial superoxide production and modulating autophagy in a dopaminergic cellular model (Pasban-Aliabadi *et al.,* 2013, Achour *et al.,* 2016).

Similarly to oleuropein, rutin (RUT) also improves locomotor activity, motor coordination, antioxidant level, dopamine content, dopaminergic D2 receptor number in 6-OHDA-treated rat model (Khan *et al.,* 2012). RUT protects mitochondrial functions and ameliorates neural apoptosis (Zhai *et al.,* 2016). Moreover, a recent study showed that rutin increased dopamine biosynthesis, and attenuated the apoptotic genes, which were expressed significantly in the 6-OHDA-treated neuron like PC12 cells (Magalingam *et al.,* 2016).

While the accumulating evidence supports the involvement of the benefits of OLE and RUT against neurotoxicity, the cellular and molecular mechanisms remain to be elucidated. Here we hypothesized that OLE or RUT would change ROS-induced alterations in ER- and mitochondria-associated neurodegeneration induced by 6-OHDA exposure in differentiated PC12 cells.

Materials and methods

Materials

PC12 cells were obtained from American Type Culture Collection (Manassas, VA, USA). Oleuropein and Rutin were purchased from AppliChem GmbH (Saxony-Anhalt, Germany). Fetal bovine serum (FBS), horse serum, bovine serum albumin (BSA), L-glutamine, penicillin, streptomycin, RPMI 1640 medium were purchased from HyClone (Logan, UT, USA). Mouse nerve growth factor 2.5S (2.5S mNGF) was obtained from Promega (Madison, WI, USA). Collagen Type IV from human placenta was purchased from Sigma-Aldrich (Steinheim, Germany). 6-hydroxydopamine was obtained from Tocris (Minneapolis, MN, USA). Annexin V-FITC/PI Assay Kit was obtained from eBioscience (San Diego, CA, USA). High Pure RNA Isolation Kit and High Fidelity cDNA Synthesis Kit were obtained from Roche Diagnostics (Mannheim, Germany). BCA™ Protein Assay Kit was obtained from Thermo Scientific (Waltham, MA, USA). PCR reagents were purchased from New England Biolabs (Ipswich, UK). Rabbit mono- or poly-clonal antibodies to PDI, CHOP, PERK, PDI, ATF-4, IRE1α, β-Actin were obtained from CST (Danvers, MA, USA). All other

reagents were purchased from Sigma or Millipore unless otherwise noted.

Cell culture

Neuron-like PC12 cells derived from a transplantable rat pheochromocytoma, were cultured in RPMI 1640 supplied with 2 mM L-glutamine, 100 IU/mL penicillin and 100 μg/mL streptomycin. The cultures were maintained in a 5% CO_2 95% air humidified atmosphere at 37 °C, and the culture medium was changed every 2–3 days. Cells were seeded on 100 μg/mL collagen type IV coated plates and passaged at 70–80% confluency. Cells were differantiated using RPMI 1640 media containing 1% heat-inactivated horse serum, 100 ng/mL NGF, 100 μg/mL BSA, 2 mM L-glutamine, 100 IU/mL penicillin and 100 μg/mL streptomycin. All the experiments were carried out with NGF (100 ng/mL) supplemented differentiation media.

Morphological changes and cell viability assay

Cell viability was determined by trypan blue exclusion assay. In brief, differentiated PC12 cells were seeded at a density of 2×10^4 cells/cm^2 for 24 h at 37 °C and then incubated with various concentrations of OLE or RUT (1, 10, 50, 100, 200, 250, 500 μM) for 24 h or 6-OHDA (100 μM) for 8 h, 12 h, 24 h. For protection experiments of OLE and RUT, cells were pre-incubated with OLE or RUT with various concentrations (1, 10, 50, 100 μM) for 6 h, followed by 8 h 100 μM of 6-OHDA treatment. After the incubation period, the cells were trypsinized and then stained with trypan blue (0.4%), and viable cells were counted using a hemocytometer. For morphological changes after treatments, cell images were captured using Leica DM6000 microscope with a Leica DFC420 camera.

Flow cytometry analysis

Apoptosis and necrosis were determined using an Annexin V-FITC/PI Assay Kit according to the manufacturer's protocol. Briefly, cells were trypsinized after treatments, washed twice with cold PBS, and then re-suspended in binding buffer at a density of 1×10^5 cells/mL. After incubation with 5 μL of Annexin V-FITC and 5 μL of propidium iodide (PI) working solution in dark for 15 min at room temperature, the cells were washed and analyzed by FacsCalibur Flow Cytometer (Becton-Dickinson) using Cell Quest software (Becton-Dickinson, San Jose, CA). FITC Annexin V positive and PI negative cells were considered as early apoptotic; however both FITC Annexin V and PI positive cells were defined as late apoptotic or necrotic cells.

Assessment of mitochondrial membrane potential (ΔΨm)

ΔΨm was determined using a JC-1 dye. The cells were seeded in 24-well plates at a density of 5×10^4 cells/well. To assess the integrity of ΔΨm, the cells were pre-treated with OLE and RUT in different concentrations (1, 10, 50 μM) for 6 h, followed by 100 μM of 6-OHDA treatment for 8 h and then stained with 10 μM JC-1 at 37 °C for 30 min in darkness. Then the cells were washed twice with PBS. The JC-1 fluorescence images were captured and processed using Leica LAS AF7000 software. Images were analyzed in terms of fluorescence integrities and the ratios of red (non- apoptotic cells)/green (apoptotic cells) were calculated by Image J Software (NIH Image, USA) compared with control and 6-OHDA treated cells.

RNA extraction and cDNA synthesis

Differentiated PC12 cells were seeded in 6-well plates at a density of 5×10^5 cells/well. Cells were pre-treated with OLE or RUT in different concentrations (1, 10, 50 μM) for 6 h. After pre-treatments, the cells were incubated with 100 μM of 6-OHDA for 8 h. Also Thapsigargin was used as a positive control as an ER-stress inducer at 300 nM for 8 h. Total RNA extraction was performed using High Pure RNA Isolation Kit according to the kit protocol. RNA quantity/quality was measured with Nanodrop ND-Spectrophotometer Lite (Thermo Scientific, USA) and was also confirmed by gel electrophoresis containing 1.5% agarose. cDNA synthesis, based on reverse transcription reactions, was performed with 1 μg of RNA and High Fidelity cDNA Synthesis Kit which contains 2.5 μM random hexamer, 1× transcriptor High Fidelity Reverse Transcriptase reaction buffer, 20 U protector Rnase inhibitor, 1 mM deoxynucleotide mix, 5 mM DTT, 10 U Transcriptor High Fidelity Reverse Transcriptase at final concentration. The following incubation conditions were applied; 10 min at 65 °C, 30 min at 55 °C and 5 min at 85 °C.

Reverse Transcription PCR (RT-PCR)

Amplification with XBP-1 and β-ACTIN primer couples were performed with the following thermal cycling conditions: denaturation for 5 min at 95 °C; 35 cycles of 15 s at 95 °C, 15 s at 59 °C, and 15 s at 72 °C; and an elongation step of 7 min at 72 °C. The primers were β-ACTIN (For-CCCGCGAGTACAACCTTCT; Rev-CGTCATCCATGGCGAACT), XBP1 (For-TTACGAGAGAAAACTCATGGGC; Rev-GGGTCCAACTTGTCCAGAATGC). The final concentrations of the PCR reagents for each type of PCR were: Phusion HF buffer, 0.2 mM dNTPs, 10 pM forward and reverse primers and 2 units of Phusion DNA Polymerase per reaction.

Agarose gel electrophoresis

For the splice variant analysis of XBP1 gene transcripts, RT-PCR products were separated electrophoretically using 2.5% agarose gel containing 0.5 μg/mL ethidium bromide. For the agarose gel electrophoresis, TAE (Tris, acetic acid, EDTA) buffer consists of 40 mM Tris, 20 mM acetic acid, and 1 mM EDTA (pH 8) was used as the gel running buffer. For the sizing of the restriction fragments, 2-Log DNA Ladder was used as the size standard. Restriction fragments (Unspliced XBP-1= 289 bp, Spliced XBP-1= 263 bp) were visualized using UV transilluminator and their relative densities were calculated by Image J Software (NIH Image, USA).

Protein extraction and Western Blot analysis

After each treatment and induction, the cells were washed twice with ice-cold PBS and centrifuged at 2000 rpm

for 10 min. Cell pellets were lysed by lysis buffer (RIPA) containing protease and phosphatase inhibitor cocktails and incubated on ice for 30 min. After centrifugation at 12,000 *g* for 15 min at 4 °C, the supernatant was separated and the protein content of each sample was determined by BCA™ Protein Assay Kit according to the manufacturer's protocol. 30 μg of lysates were loaded onto a 10 % sodium dodecyl sulfate-polyacrylamide gel electrophoresis (SDS-PAGE) for 1.5 h at 100V and and transferred onto 0.2 μm nitrocellulose membranes. After blocking with 5% non-fat milk in TBST (Tris-buffer saline with 0.1% Tween 20) buffer for 1 h at room temperature. Membranes were incubated overnight at 4 °C with primary antibodies against PDI, CHOP, PERK, PDI, ATF-4, IRE1α and β-Actin as an internal control. After being washed with TBST three times, the membranes were probed with an appropriate horseradish peroxidase (HRP)-conjugated secondary antibody for 2 h at room temperature. Blots were developed using electrochemiluminescence (ECL) reagent and detected using an ECL system (Gel Logic 2200 PRO Imaging System, Carestream, USA). The band intensities were quantified with Image J software (NIH Image, USA). All experiments were performed in triplicate.

Statistical analysis

Statistical analysis was performed with the unpaired Student's *t*-test for viability assay. One-way analysis of variance (ANOVA) with Bonferroni post hoc test for flow cytometry analysis and Holm Sidak post hoc tests were performed for other parameters using SigmaStat v3.5 software. The results were expressed as mean values ± SEM and values of $p<0.05$, $p<0.01$ and $p<0.001$ were considered statistically significant.

Results

Morphology and the viability of PC12 cells

PC12 cell morphology was observed under inverted phase contrast microscope and cell mortality calculated by trypan blue assay. Control neuron like PC12 cells grew in a high density with long neurites and intact morphology (Figure 1A), but exposure to 6-OHDA (100 μM) led to formation of short neurites, decadent neuronal network swelling and impaired membrane integrity, in a time dependent manner (8–24 h) (Figure 1B–D). In contrast to 12–24 h incubation time with 6-OHDA, differentiated PC12 cell morphology still tended to outgrow neurites, and so they did 8 h after incubation with 100 μM concentration of 6-OHDA (Figure 1B). OLE or RUT pretreated cells had greater tendency to increase neurite outgrowth and showed a few changes on the morphology when compared to the cells exposed to 6-OHDA alone (Figure 1E–L). The trypan blue exclusion assay displayed a gradually decreased viability after increasing concentration of 6-OHDA (data not shown). In accordance with the results of the imaging study, the cell viability decreased around 50% after 8 h treatment with 6-OHDA (100 μM) (*vs* control cells $p<0.001$). Figure 1M shows the cell viability results obtained from pretreatment with increasing concentrations of OLE or RUT (1–500 μM) for 24 h. OLE or RUT progresivelly inhibited cell viability at high concentrations (100–500 μM). Figure 1N shows the effects of pretreatment with increasing concentrations (1, 10, 50, 100 μM) of OLE or RUT for 6 h on 6-OHDA (100 μM; 8 h) treated cells. OLE or RUT at relatively low concentrations caused a significant normalization in the viability of cells exposed to 6-OHDA (*vs* 6-OHDA treatment alone $p<0.001$).

Effects of OLE and RUT on 6-OHDA-induced cell apoptosis.

Effects of OLE and RUT on 6-OHDA-induced cytotoxicity were also evaluated by Annexin V-FITC/PI assay. The results showed that 11.58% of control cells were apoptotic and 5.70% of them were necrotic (Figure 2B, J and K). In the 6-OHDA exposed group (100 μM 8 h), many apoptotic nuclei positive for PI staining were observed, and the apoptotic and necrotic cell ratios were significantly increased up to 57% and 15.10%, respectively (*vs* control cells $p<0.001$) (Figure 2C, J and K). However, the number of apoptotic nuclei was decreased in pretreated groups. Pretreatment of the cells with OLE or RUT with 1, 10, 50 μM for 6 h, significantly reduced AV (+) cells to 13.70%, 13.10% and 16.75% for OLE (Figure 2D, E and F) and 13.45%, 15.00% and 19.10% for RUT (Figure 2G, H and I), respectively (*vs* control cells $p<0.001$) (Figure 2J, K). As shown in Figure 2K, OLE or RUT in all concentrations significantly decreased PI (+) cells, and this effect was observed as more significant in the presence of 1 μM of RUT and 1 μM or 50 μM of OLE (*vs* 6-OHDA or control group $p<0.001$).

Effects of OLE and RUT on mitochondrial membrane potential

Mitochondrial membrane potential (ΔΨm) is critical for maintaining the physiological function of the respiratory chain to generate ATP (Joshi & Bakowska, 2011). Mitochondrial membrane potential was measured by fluorescence staining with JC-1 dye. JC-1 is aggregated in mitochondria in living cells and emits red fluorescence, but in apoptotic cells JC-1 remains in the monomeric form, which shows green fluorescence. As shown in Figure 3A, the control group of cells emitted more intense red fluorescence. After being treated with 6-OHDA, the red fluorescence intensity was decreased and the green was increased (Figure 3B), while the cells were able to overcome 6-OHDA–induced green fluorescence intensity when pretreated with OLE or RUT (Figure 3C and 3F). However, the cells were tending to undergo apoptosis and emitted green fluorescence at high concentrations of phytochemicals compared to control cells. The results of JC-1 experiments showed that 6-OHDA treatment significantly decreased red/green fluorescence ratio that could be prevented by pretreatment with OLE or RUT ($p<0.01$). In case of pre-treatment with low concentration of OLE (1 μM), red fluorescence intensity was similar to the red fluorescence intensity obtained from control cells, and there was no significant difference (Figure 3I). But, as shown in Figure 3D and 3E, the red/green

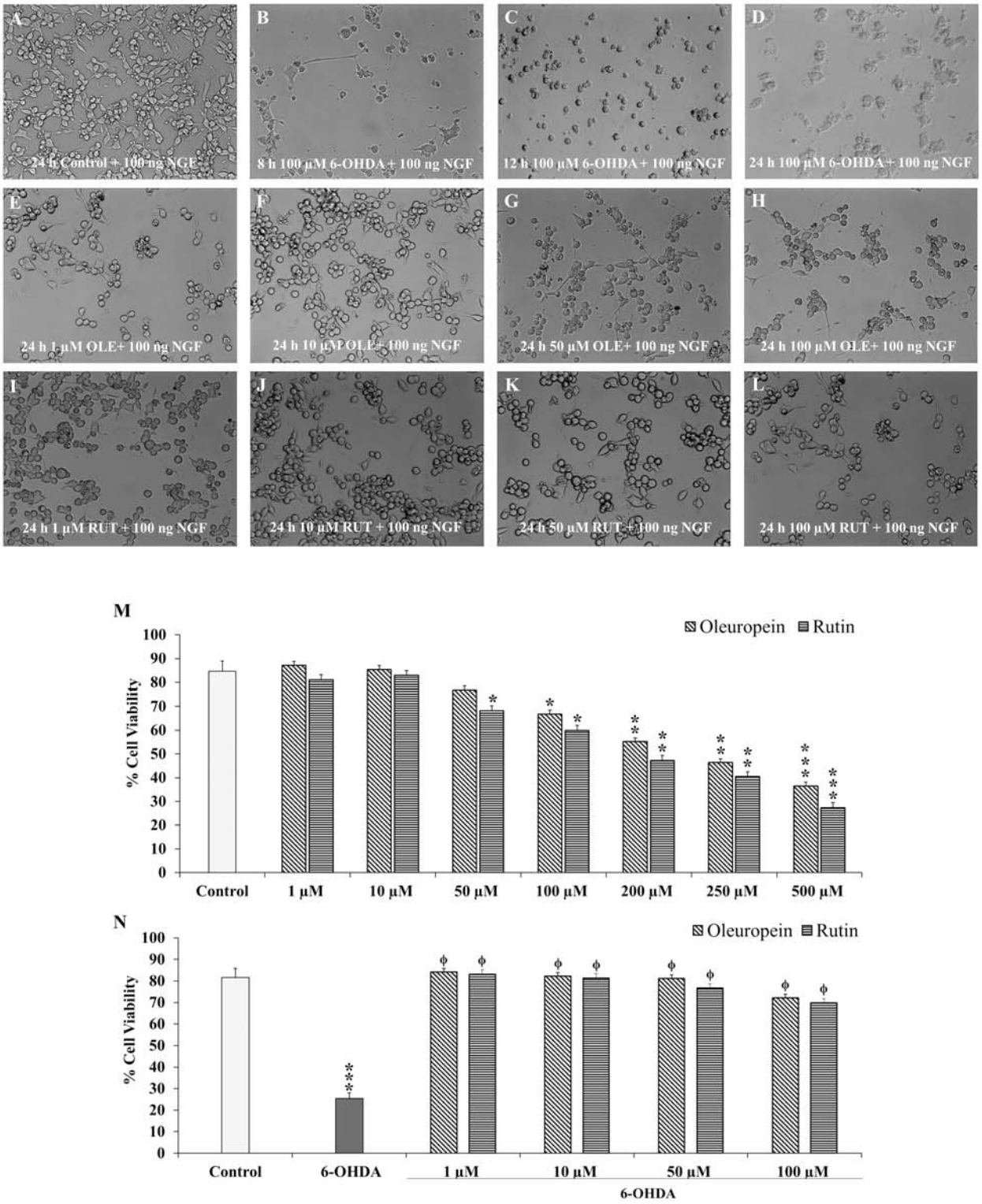

Figure 1. Representative morphological images of PC12 cells under phase-contrast microscopy (A–L) (Magnification: 400x). Control cells were treated with NGF (100 ng/mL) for 24 h (A). NGF (100 ng/mL)-stimulated cells were treated with 100 µM 6-OHDA for 8, 12, 24 h (B–D), various concentrations (1, 10, 50, 100 µM) of OLE or RUT for 24 h (E–L). Effects of OLE and RUT were assessed by trypan blue exclusion assay; cells were treated with OLE or RUT with various concentrations (1, 10, 50, 100, 200, 250, 500 µM) for 24 h (M), and cells were pre-treated with OLE or RUT with various concentrations (1, 10, 50, 100 µM) for 6 h, then post-treated with 100 µM of 6-OHDA for 8 h (N). The assay was performed as described in Materials and Methods section. Data were expressed as mean ± SEM; n=6 wells per each group. Statistical significance was determined with unpaired Student's *t*-test, ***$p<0.001$, versus control cells. $\Phi p<0.001$, versus 6-OHDA treated cells. 6-OHDA: 6-hydroxydopamine; OLE: Oleuropein; RUT: Rutin; NGF: Nerve growth factor.

fluorescence ratio was decreased significantly when the cells were pretreated with 10 µM or 50 µM OLE (p<0.01). In all concentrations of RUT, red fluorescence intensity was significantly decreased (*vs* control group p<0.05 for 1 µM and 10 µM RUT; p<0.01 for 50 µM RUT) (Figure 3F, G and H).

Effects of OLE and RUT on the expression of ER stress-related proteins in 6-OHDA-induced neuron-like PC12 cells

To investigate the involvement of ER stress in the neuroprotective effect of OLE and RUT, we measured the expressions of ER stress markers with Western blot (Figure 4). 6-OHDA (100 µM) treatment increased CHOP protein expression in a time dependent manner, and CHOP levels reached maximal level after 8 h of incubation with 6-OHDA (2.5-fold) (*vs* time 0 h p<0.001) (Figure 4A). We show that OLE and RUT, when used at relatively low concentrations (1, 10, 50 µM) decreased 6-OHDA induced CHOP increment (*vs* 6-OHDA p<0.01). On the other hand, ER stress responsive kinase IRE1α levels and ATF-4 translational expression were significantly up-regulated by 6-OHDA treatment (100 µM; 8 h) (*vs* control p<0.001) (Figure 4B, C). Interestingly, all pre-treatment regimens were able to produce a further increase in this UPR (*vs* 6-OHDA alone p<0.05-p<0.001) (Figure 4C). Only 50 µM RUT had no significant effect on IRE1α protein levels in 6-OHDA-induced neuron-like PC12 cells.

Moreover, PERK, PDI and BIP protein levels were decreased by 6-OHDA treatment (100 µM; 8 h) (*vs* control p<0.001), and OLE and RUT when used at relatively low concentrations (1, 10, 50 µM) produced a further decline in 6-OHDA-induced reduction in PERK, PDI and BIP protein levels (*vs* 6-OHDA alone p<0.05-p<0.01). Especially at 10 and 50 µM concentrations of RUT, 2.7- and 2.94-fold decrease in PERK level as well as 2.2- and 2.1-fold decrease in PDI level (vs 6-OHDA alone p<0.01) were observed (Figure 4D).

Effects of OLE and RUT pretreatment on the splice variant of XBP1 in 6-OHDA-induced differentiated PC12 cells

To evaluate whether 6-OHDA-induced apoptosis in PC12 cells or the effects of OLE or RUT is related to XBP1S associated ER stress, we measured XBP1 splice variant (XBP1S) levels semi-quantitatively, by agarose gel electrophoresis. Thapsigargin was used as a positive control for induction of the splicing of XBP-1 in PC12 (data not shown). A significant up-regulation of XBP1 splicing was observed following treatment with 100 µM 6-OHDA. Pretreatment with 1–10 µM OLE or 1 µM RUT followed by 6-OHDA treatment resulted in lowered XBP1S variant levels, (*vs* 6-OHDA alone p<0.05, p<0.001, respectively) (Figure 5B). However, 50 µM OLE or 10 µM RUT did not change 6-OHDA-induced splicing of XBP1 (*vs* 6-OHDA alone p>0.05) (Figure 5B).

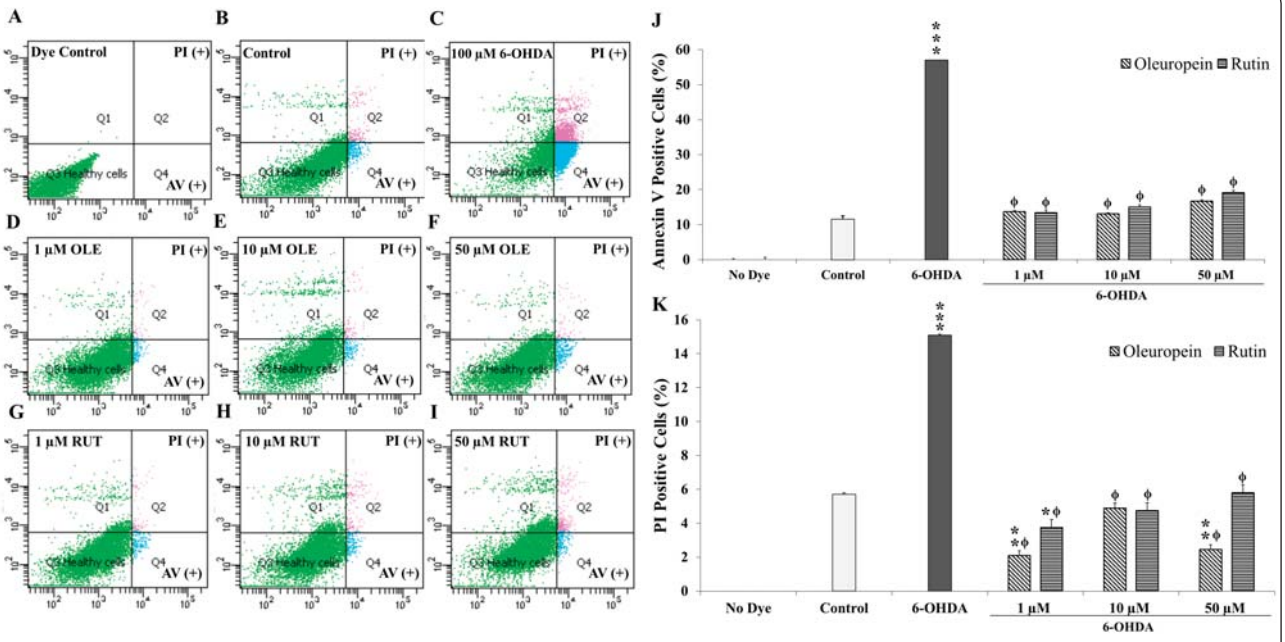

Figure 2. Flow cytometry analysis of NGF (100 ng/mL)-stimulated PC12 cells using Annexin V-FITC and propidium iodide, and the results were expressed as in the dot plots (A–I). No dye group cells (without staining AV and PI dye) were treated only with NGF (100 ng/mL) for 24h (A). Control cells were treated with NGF (100 ng/mL) (B). NGF (100 ng/mL)-stimulated cells were treated with 100 µM 6-OHDA for 8 h (C), various concentrations (1, 10, 50 µM) of OLE or RUT for 6 h then post-treated with 8 h 100 µM of 6-OHDA (D–I). Effects of OLE and RUT were assessed by evaluating AV (+) and PI (+) cell ratios, as described in Materials and Methods section (J–K). Data were expressed as mean ± SEM; n=4–5 wells per each group. Statistical significance was determined with one-way analysis of variance (ANOVA) with Bonferroni *post hoc* test,* p<0.05, **p<0.01 ***p<0.001 versus control cells; $^{\Phi}p$<0.001 versus 6-OHDA treated cells. 6-OHDA: 6-hydroxydopamine; OLE: Oleuropein; RUT: Rutin; AV: Annexin V; PI: Propidium iodide.

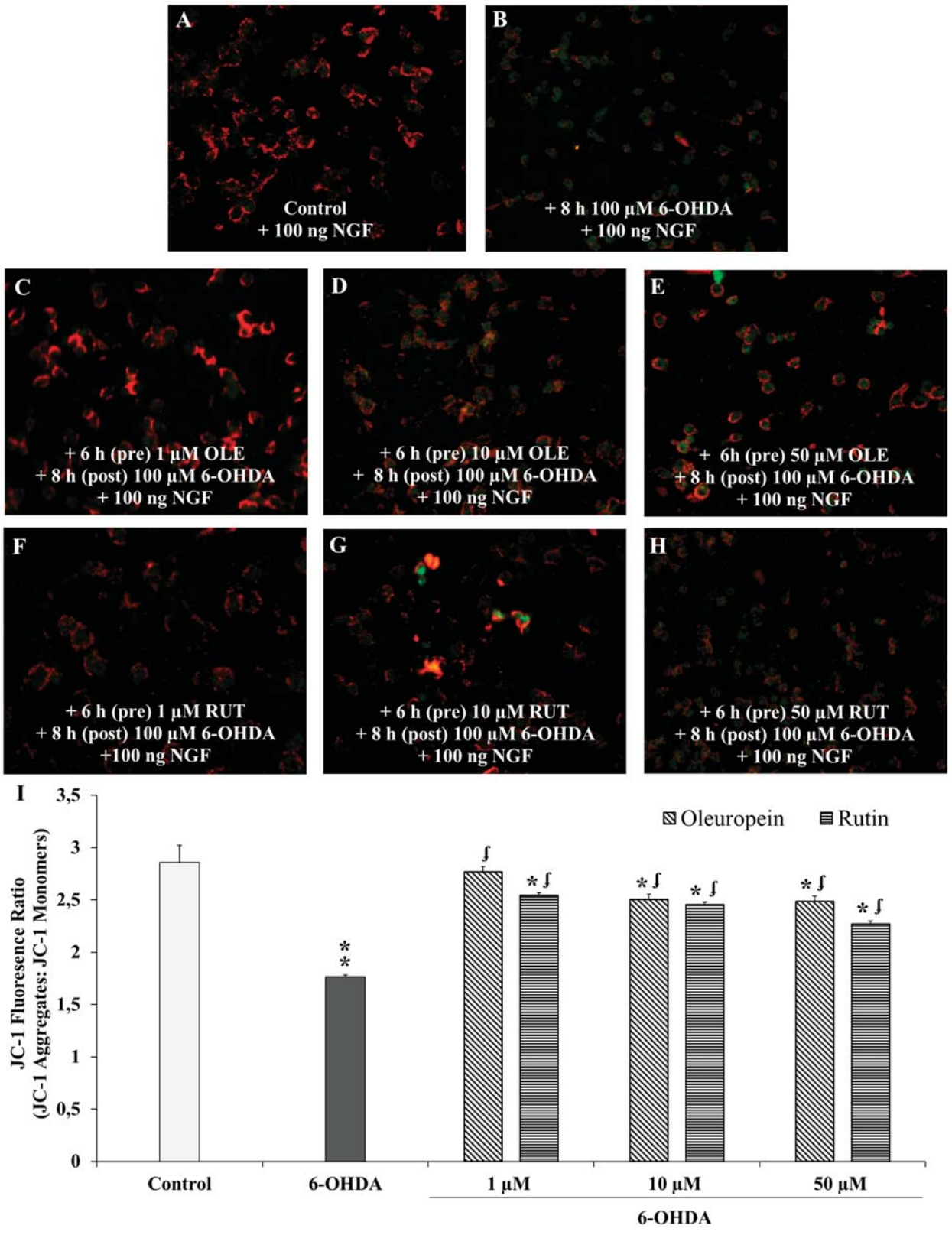

Figure 3. JC-1 staining for 6-OHDA-induced dissipation of mitochondrial membrane potential NGF (100 ng/mL)-stimulated PC12 cells (A–I) (Magnification: 400X). NGF (100 ng/mL)-stimulated cells were treated with 100 µM 6-OHDA for 8 h (C), various concentrations (1, 10, 50 µM) of OLE or RUT for 6 h then post-treated with 100 µM of 6-OHDA for 8 h and stained for 30 min with JC-1, a mitochondrial potential sensitive dye (A–H). Fluorescence patterns of different antioxidant groups, as represented in the pictures, were increased in red JC-1 aggregates; increase in green fluorescence means attenuation of mitochondrial membrane potential. Data (red/green fluorescence ratios) were expressed as mean ± SEM; n=3 wells per each group (I). Statistical significance was determined with one-way analysis of variance (ANOVA) with Holm Sidak *post hoc* test,*p<0.05, **p<0.01 versus control cells; ^{f}p<0.01 versus 6-OHDA treated cells. 6-OHDA: 6-hydroxydopamine; OLE: Oleuropein; RUT: Rutin.

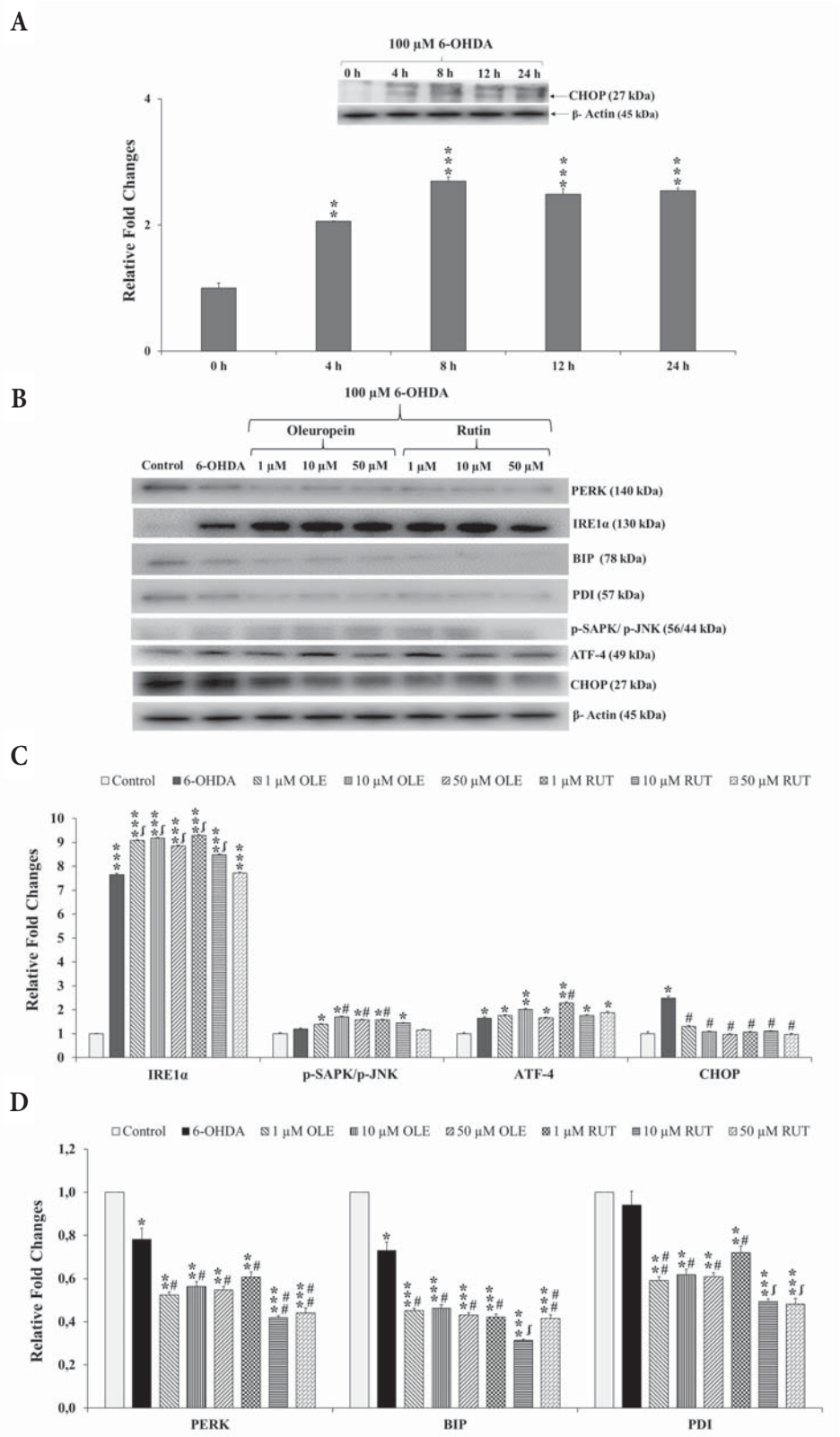

Figure 4. Effects of OLE or RUT on the ER-stress related protein levels in 6-OHDA (100 µM, 8 h)-induced and NGF (100 ng/mL)-stimulated PC12 cells were examined by western blot analysis (A, B, C, D). CHOP protein levels were examined in NGF (100 ng/mL)-stimulated PC12 cells treated with 100 µM 6-OHDA for 4, 8, 12, 24 h (A). Each value represents the mean ± SEM band density ratio for each group (n=3). β-Actin was used as an internal control (A, B, C, D). Statistical significance was determined with one-way analysis of variance (ANOVA) with Holm Sidak post hoc test, *p<0.05, **p<0.01 and ***p<0.001 versus control cells or time 0 h cells ; $^{\#}p$<0.05, $^{\#\#}p$<0.01 and ^{ſ}p<0.001 versus 6-OHDA treated cells. 6-OHDA: 6-hydroxydopamine; OLE: Oleuropein; RUT: Rutin; PERK: Protein kinase R (PKR)-like endoplasmic reticulum kinase; IRE1α: inositol-requiring enzyme 1α; BIP: binding immunoglobulin protein; PDI: protein disulfide-isomerase; ATF-4: activating transcription factor 4; CHOP: C/EBP-homologous protein.

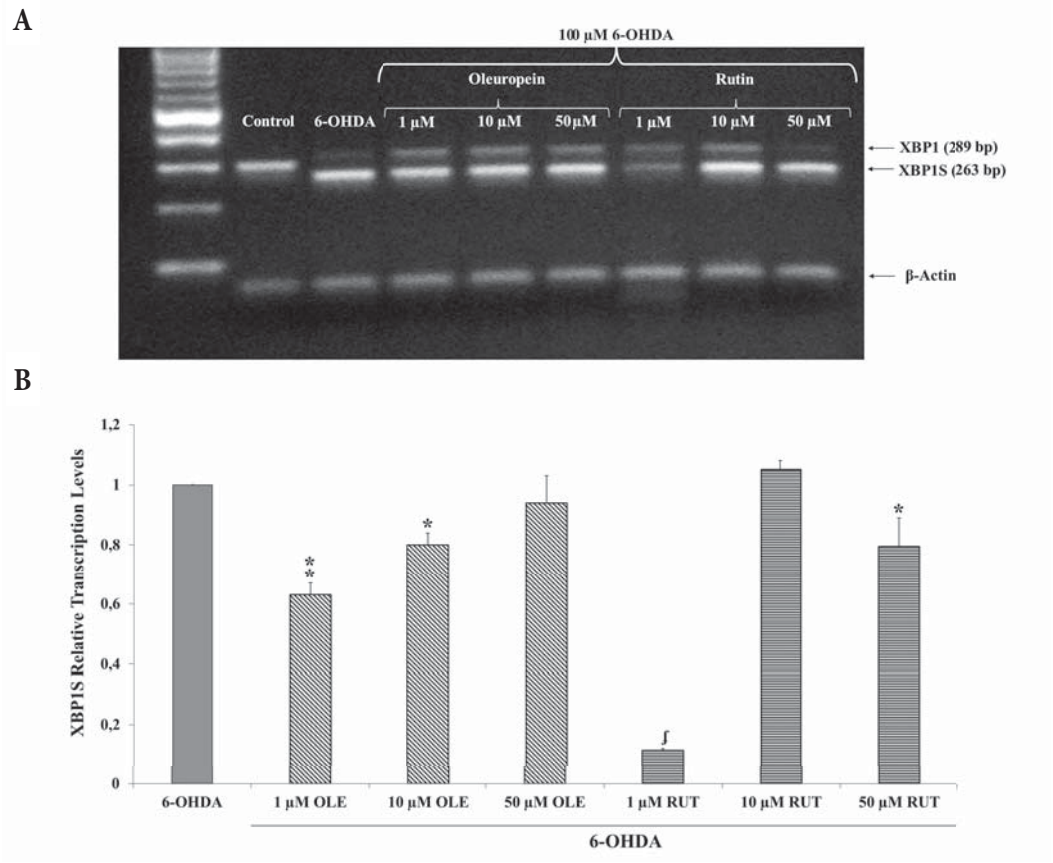

Figure 5. Effects of OLE and RUT on XBP1S transcription levels in 6-OHDA-treated PC12 cells (A, B). Data were expressed as mean ± SEM; n=3 wells per each group. Statistical significance was determined with unpaired Student's t-test, *p<0.05, **p<0.01 and ^{f}p<0.001 versus 6-OHDA treated cells. 6-OHDA: 6-hydroxydopamine; OLE: oleuropein; RUT: rutin; XBP1: X-box binding protein 1: XBP1s: X-box binding protein 1 splice variant.

Discussion

Most neuroprotective antioxidants have hormetic properties and interact with cell signaling systems to modulate adaptive stress responses via changing gene expression of various stress responsive proteins (Joshi & Bakowska, 2011). Numerous polyphenolic antioxidants as well as OLE or RUT have shown therapeutic potential against neurodegenerative diseases (Calabrese *et al.,* 2010; Barbaro *et al.,* 2014; Rodríguez-Morató *et al.,* 2015; Magalingam *et al.,* 2016). However, the underlying cellular and molecular mechanisms are largely unknown. In this study, we investigated the action mechanisms of OLE and RUT on 6-OHDA-induced neurodegeneration in differentiated PC12 cells, and we provided direct evidence to indicate that hormetic effect and the related signaling pathways were responsible for the neuroprotective activity of both OLE and RUT.

In fact, the characteristic of hormesis is a biphasic dose-response with a low dose stimulatory/beneficial effect (improved function, increased resistance to injury) and a high dose inhibitory/toxic effect (dysfunction, molecular damage, or even death) (Rieger *et al.,* 2011). Hormesis in the nervous system has been documented as neurohormesis (Mattson & Cheng, 2006), which is regulated by plant secondary metabolites (Zhang *et al.,* 2016), neurotoxins and other endogenous factors. It activates compensatory pathways to induce neuroprotection, neurite outgrowth and cell viability (Zhang *et al.,* 2017; Murugaiyah & Mattson, 2015). We found that both OLE and RUT produce typical neurohormetic dose-response effects in NGF-differentiated PC12 cells, a rat pheochromocytoma cell line with typical neuron features, that has been widely introduced as a neuronal cell *in vitro* model (Rieger *et al.,* 2011). Differentiated PC12 cells when preincubated with OLE or RUT at the concentrations ranging from 1–50 µM significantly ameliorated 6-OHDA-induced growth inhibition. The neuroprotective effect of OLE and RUT was confirmed by flow cytometry measurements, and we found that the pretreatment with OLE or RUT at hormetic concentrations (1–50 µM) inhibited 6-OHDA-induced neuronal apoptosis. However, the relatively high concentrations of OLE and RUT (100–500 µM) did not produce a protective activity, but inhibited cell viability and enhanced cytotoxicity of 6-OHDA. In accordance with our findings, previous studies reported that 6-OHDA-induced cell death involves apoptotic and necrotic features (Li *et al.,*

2015), and OLE, olive leaf extract (Pasban-Aliabadi *et al.,* 2013) and also RUT (Magalingam *et al.,* 2016) are able to inhibit 6-OHDA-induced neuron-like PC12 cell apoptosis. Moreover, Martín-Aragón *et al.* reported that RUT and quercetin might have neuroprotective effects on SH-SY5Y cell line, over-expressing the amyloid precursor protein, through their neurohormetic effects via modulating proteasomal function (Martín-Aragón *et al.,* 2016). 6-OHDA has been demonstrated to cause mitochondrial damage by effecting mitochondrial dynamics, leading to excess production of ROS and the activation of ROS-mediated cellular death pathways (Magalingam *et al.,* 2016). In this context, mitochondrial membrane potential (ΔΨm) is a key indicator for evaluating mitochondrial dysfunction, and the loss of ΔΨm indicates overproduction of ROS (Joshi & Bakowska, 2011). Mitochondrial dysfunction contributes to apoptosis induction and plays a central role in 6-OHDA-activated cell death (Zuo and Motherwell, 2013; Hu *et al.,* 2014; Jha *et al.,* 2017). Accordingly, our results demonstrated that the treatment with 100 µM 6-OHDA during 8 h resulted in a sharp loss of ΔΨm. However, pretreatment with OLE or RUT (1–50 µM) attenuated 6-OHDA-induced loss in ΔΨm and promoted neuronal survival in consistency with the findings from our flow cytometry experiments. The ΔΨm protecting effect of OLE or RUT has been demonstrated previously in diferent cell models of oxidative stress (Cumaoglu *et al.,* 2011a, 2011b; Carrasco-Pozo *et al.,* 2012).

On the other hand, excess ROS production due to impaired mitochondrial integrity is a major reason of UPR and ER stress that can also trigger mitochondrial damage by altering protein folding enzyme functions which, in turn, leads into ER stress again. This crosstalk between ER stress and mitochondrial dysfunction is induced by 6-OHDA both directly and indirectly (Cai *et al.,* 2016). Accumulation of misfolded proteins within the ER activates UPR, resulting with the execution of adaptive or non-adaptive signaling pathways (Benyair *et al.,* 2011; Hoozemans & Scheper, 2012). Upon activation, the UPR orchestrates cellular alterations in transcription, translation and protein degradation. These changes are mediated through the activation of three well-known sensors of the UPR, inositol-requiring protein 1 alpha (IRE1α), PKR (double-stranded-RNA-dependent protein kinase)-like ER kinase (PERK), activating transcription factor-6 (ATF6) and their downstream effectors (Cai *et al.,* 2016). Their activation triggers specific adaptive responses to resolve the stress or initiates signalling pathways that lead to apoptosis, depending on the severity and duration of the stress (Hosoi & Ozawa, 2009; Leitman *et al.,* 2013;

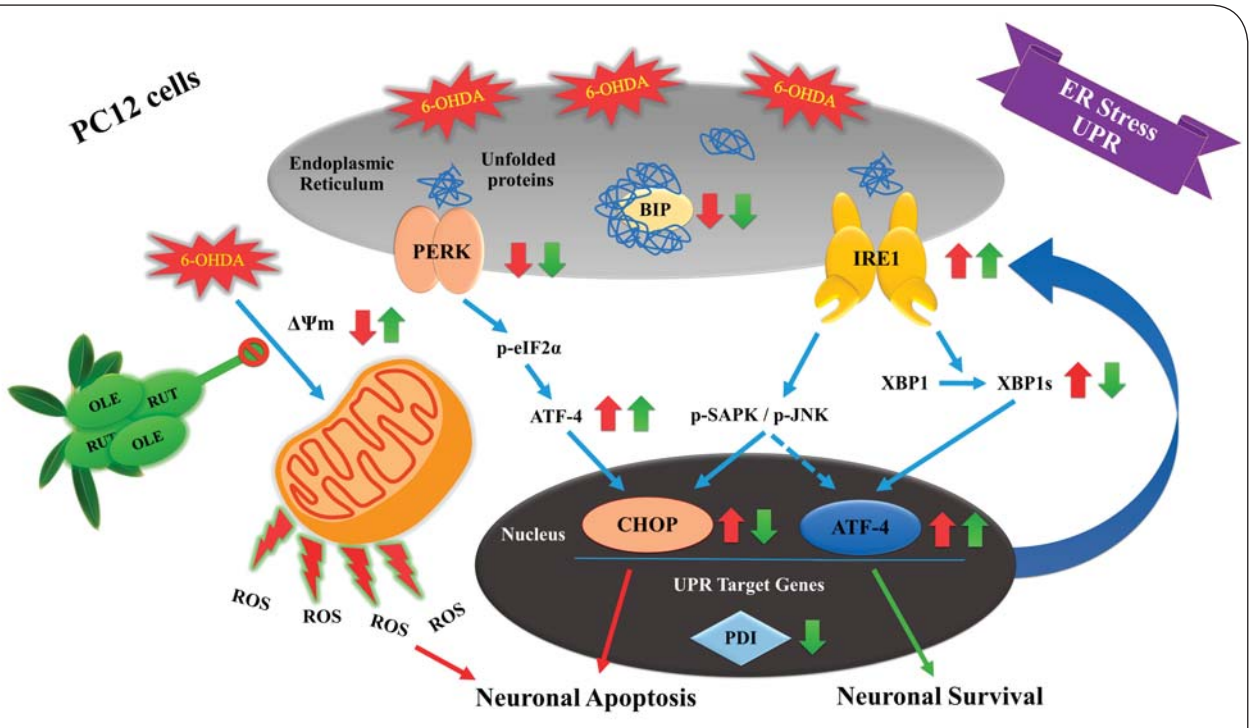

Figure 6. Mechanistic insight of OLE and RUT in preventing 6-OHDA-induced ER-stress in PC12 cells. 6-OHDA induces both mitochondrial dysfunction and ER-stress, leading to over-production of ROS and unfolded protein response (UPR). OLE and RUT attenuate 6-OHDA induced adaptive response to survival via directly regulating mitochondrial functions, promoting IRE1α signaling pathway (ATF-4), reducing ER protein overload (via PERK, BIP, PDI downregulation); rather than apoptosis (CHOP, ROS overproduction). OLE and RUT can also enhance stress related pathways under serum deprivation concomitantly with 6-OHDA exposure, however cell viability and healthy-apoptotic cells ratio remain elevated. Red arrows: 8 h 100 µM 6-OHDA alone treatment; green arrows: 6 h OLE or RUT pre-treatment, followed by 8 h 100 µM 6-OHDA treatment. 6-OHDA: 6-hydroxydopamine; OLE: Oleuropein; RUT: Rutin; UPR: Unfolded protein response; PERK: Protein kinase R (PKR)-like endoplasmic reticulum kinase; IRE1α: Inositol-requiring enzyme 1α; XBP1: X-Box binding protein 1; XBP1s: X-Box binding protein 1 splice variant; BIP: Binding immunoglobulin protein; PDI: Protein disulfide-isomerase, SAPK/JNK: Stress-activated protein kinase/Jun-amino-terminal kinase; ATF-4: Activating transcription factor 4 CHOP: C/EBP-homologous protein; ΔΨm: Mitochondrial membrane potential; ROS: Reactive oxygen species.

Credle *et al.,* 2015; Cai *et al.,* 2016). Once, ER-stress is activated, a chaperone protein named binding immunoglobulin protein (BIP) dissociates from misfolded proteins and activates IRE1α and PERK. Incubation of differentiated PC12 cells with 100 μM dose of 6-OHDA induced UPR in a time dependent manner (0, 4, 8, 12, 24 h) that was determined by increased levels of UPR signaling molecule CHOP (via IRE1α but not PERK). In UPR cascade, the activation of PERK via phosphorylation leads to the phosphorylation of eukaryotic initiation factor 2 (eIF2α) to induce translational repression in order to decrease ER overload (Kondratyev *et al.,* 2007; Leitman *et al.,* 2013). If eIF2α severely decreases, the activating protein-4 (ATF-4) is induced, which promotes apoptotic ER-stress marker C/EBP homologous protein (CHOP) (Ogen-Shtern *et al.,* 2016). Although we did not evaluate the phosphorylation level of PERK, its documented decreased total levels following 6-OHDA treatment indicated that PERK was less likely to have a function as a master regulator of apoptosis in our model of 6-OHDA-induced UPR. However, we confirmed the upregulated levels of ATF-4 and CHOP, a major transcription factor mediating ER-stress-induced apoptosis which, in accordance with previous study (Szegezdi *et al.,* 2006), settled at maximum level after 8 h of incubation with 6-OHDA. Furthermore, phosphorylated IRE1α activates SAPK/JNK pathways (Muralidharan & Mandrekar, 2013) and also induces inactive X-box-binding protein 1 (XBP1) mRNA splicing to its active XBP1S variant. We found that 6-OHDA-induced UPR increases XBP1 splicing, which can promote adaptive or apoptotic ER stress-related genes. In fact, ATF-4 not only regulates the expression of pro-apoptotic gene CHOP under chronic stress conditions (Galehdar *et al.,* 2010; Mercado *et al.,* 2015), but also translocates to the nucleus where it induces the expression of ER chaperones, such as protein disulfide isomerase (PDI), which increases refolding of misfolded proteins (Halperin *et al.,* 2014). PDI, a convergent center of ER redox homeostasis and signalling processes (Zeeshan *et al.,* 2016) has been suggested to occur as an early adaptive response in toxin-mediated stress (Kim-Han & O'Malley, 2007). In the cellular model of the PD, the increased oxidative modification of PDI has been reported to result in inhibition of its activity, triggering ER stress and possibly cell death (Mercado *et al.,* 2013). Consistently with previous observations (Mercado *et al.,* 2015), we found an unchanged PDI protein level in 6-OHDA treated neuron-like PC12 cells. On the other hand, BiP is a HSP70 molecular chaperone located in the lumen of the ER that binds newly synthesized proteins as they are translocated into the ER and maintains them in a state competent for subsequent folding and oligomerization. Under ER stress, the cells activate BiP, which protects them from lethal conditions (Schroder & Kaufman, 2005). In the present study, inhibited BiP levels were associated with unchanged PDI levels in 6-OHDA treated cells. A previous study suggested that UPR-mediated apoptosis or survival is dependent on the balance between BIP and CHOP levels, and 6-OHDA exposure induces CHOP rather than BIP (Hu *et al.,* 2014). In accordance with all findings, our differentiated PC12 cells underwent apoptosis via the CHOP pathway due to continuous 6-OHDA-induced ER stress. Another interesting finding of this study is the effect of OLE and RUT on 6-OHDA-induced UPR. We found that pretreatment with OLE or RUT leads to potentiation of 6-OHDA-induced increases in the levels of IRE1α and ATF-4, but not CHOP. CHOP was significantly inhibited by OLE or RUT pretreatment, consistently with the results of our flow cytometry experiments. Sun *et al.* suggested that ATF-4 overexpression influences different proteins that in turn regulate parkin turnover and make cells resistant to ER stressors (Sun *et al.,* 2013). Moreover, recent studies reported that IRE1α expression is inducible through ATF4 that catalyses the splicing of the XBP1, leading to neuroprotection (Tsuru *et al.,* 2016). In the light of previous works, our results suggested that preconditioning with OLE or RUT triggers adaptive response processes and increased IRE1α could potentiate ATF-4-mediated neuronal survival. Spliced XBP1 is a stable transcription factor which translocates to the nucleus to induce the upregulation of ER chaperones and proteins involved in the ER-associated degradation (ERAD) pathway (Tsai & Weissman, 2010). XBP1 also controls phospholipid synthesis which is important for ER membrane expansion when the ER is under stress (Zeeshan *et al.,* 2016). It has been demonstrated that a down-regulation of XBP1 mRNA levels triggers CHOP-mediated apoptosis and causes spontaneous neurodegeneration in adult mice nigral dopaminergic cells (Lee *et al.,* 2003; Valdés *et al.,* 2014). However, Choi *et al.* reported that baicalein induces protection in ER stress induced HT22 cells via diminishing the cleavage of XBP1 (Choi *et al.,* 2010). We found that the induction of XBP1 by 6-OHDA is inhibited by hormetic doses OLE or RUT, indicating that OLE and RUT direct the cells to adaptive state rather than irreversible apoptotic state. The present findings are in consistency with the results of a recent study, which showed that rutin protects neuron-like PC12 cells against 6-OHDA induced cytotoxicity by suppression of lipid peroxidation and activation of antioxidant enzymes (Magalingam *et al.,* 2016).

Conclusion

In summary, we demonstrated that low doses of OLE or RUT show hormetic effects and thereby neuroprotection against 6-OHDA-induced cell growth inhibition and apoptosis through preservation of mitochondrial function and activation of UPR-mediated cell survival pathways in neuron-like PC12 cells.

Acknowledgments

This study was financially supported by the Scientific and Technological Research Council of Turkey (Grant No: 114Z46). In addition, this research was supported in part by EU-COST Action BM1203.

REFERENCES

Achour I, Arel-Dubeau AM, Renaud J, Legrand M, Attard E, Germain M, Martinoli MG. (2016). Oleuropein Prevents Neuronal Death, Mitigates Mitochondrial Superoxide Production and Modulates Autophagy in a Dopaminergic Cellular Model. *Int J Mol Sci* **17**: E1293.

Alirezaei M, Rezaei M, Hajighahramani S, Sookhtehzari A, Kiani K. (2016). Oleuropein attenuates cognitive dysfunction and oxidative stress induced by some anesthetic drugs in the hippocampal area of rats. *J Physiol Sci* **67**: 131–139.

Ataie A, Shadifar M, Ataee R. (2016). Polyphenolic Antioxidants and Neuronal Regeneration. *Basic Clin Neurosci* **7**: 81–90.

Bali EB, Ergin V, Rackova L, Bayraktar O, Küçükboyaci N, Karasu Ç. (2014). Olive leaf extracts protect cardiomyocytes against 4-hydroxynonenal-induced toxicity *in vitro*: comparison with oleuropein, hydroxytyrosol, and quercetin. *Planta Med* **80**: 984–92.

Barbaro B, Toietta G, Maggio R, Arciello M, Tarocchi M, Galli A, Balsano C. (2014). Effects of the olive-derived polyphenol oleuropein on human health. *Int J Mol Sci* **15**: 18508–24.

Benyair R, Ron E, Lederkremer GZ. (2011). Protein quality control, retention, and degradation at the endoplasmic reticulum. *Int Rev Cell Mol Biol* **292**: 197–280.

Cai P, Ye J, Zhu J, Liu D, Chen D, Wei X, Johnson NR, Wang Z, Zhang H, Cao G, Xiao J, Ye J, Lin L. (2016). Inhibition of Endoplasmic Reticulum Stress is Involved in the Neuroprotective Effect of bFGF in the 6-OHDA-Induced Parkinson's Disease Model. *Aging Dis* **7**: 336–449.

Calabrese V, Cornelius C, Mancuso C, Lentile R, Stella AM, Butterfield DA. (2010). Redox homeostasis and cellular stress response in aging and neurodegeneration. *Methods Mol Biol* **610**: 285–308.

Carrasco-Pozo C, Mizgier ML, Speisky H, Gotteland M. (2012). Differential protective effects of quercetin, resveratrol, rutin and epigallocatechin gallate against mitochondrial dysfunction induced by indomethacin in Caco-2 cells. *Chem Biol Interact* **195**: 199–205.

Casamenti F, Grossi C, Rigacci S, Pantano D, Luccarini I, Stefani M. (2015). Oleuropein Aglycone: A Possible Drug against Degenerative Conditions. *In Vivo* Evidence of its Effectiveness against Alzheimer's Disease. *J Alzheimers Dis* **45**: 679–88.

Chao Y, Wong SC, Tan EK. (2014). Evidence of inflammatory system involvement in Parkinson's disease. *Biomed Res Int* **2014**: 308654.

Cheng J, Xia X, Rui Y, Zhang Z, Qin L, Han S, Wan Z. (2016). The combination of 1α,25dihydroxyvitaminD3 with resveratrol improves neuronal degeneration by regulating endoplasmic reticulum stress, insulin signaling and inhibiting tau hyperphosphorylation in SH-SY5Y cells. *Food Chem Toxicol* **93**: 32–40.

Choi JH, Choi AY, Yoon H, Choe W, Yoon KS, Ha J, Yeo EJ, Kang I. (2010). Baicalein protects HT22 murine hippocampal neuronal cells against endoplasmic reticulum stress-induced apoptosis through inhibition of reactive oxygen species production and CHOP induction. *Exp Mol Med* **42**(12): 811–22.

Credle JJ, Forcelli PA, Delannoy M, Oaks AW, Permaul E, Berry DL, Duka V, Wills J, Sidhu A. (2015). α-Synuclein-mediated inhibition of ATF6 processing into COPII vesicles disrupts UPR signaling in Parkinson's disease. *Neurobiol Dis* **76**: 112–25.

Cumaoglu A, Ari N, Kartal M, Karasu C. (2011a). Polyphenolic extracts from Olea europea L. protect against cytokine-induced β-cell damage through maintenance of redox homeostasis. *Rejuvenation Res* **14**: 325–34.

Cumaoglu A, Rackova L, Stefek M, Kartal M, Maechler P, Karasu C. (2011b). Effects of olive leaf polyphenols against H_2O_2 toxicity in insulin secreting β-cells. *Acta Biochim Pol* **58**: 45–50.

Davie CA. (2008). A review of Parkinson's disease. *Br Med Bull* **86**: 109–27.

Deng C, Tao R, Yu SZ, Jin H. (2012). Inhibition of 6-hydroxydopamine-induced endoplasmic reticulum stress by sulforaphane through the activation of Nrf2 nuclear translocation. *Mol Med Rep* **6**: 215–9.

Dias V, Junn E, Mouradian MM. (2013). The role of oxidative stress in Parkinson's disease. *J Parkinsons Dis* **3**: 461–91.

Ebrahimi-Fakhari D, Wahlster L, McLean PJ. (2012). Protein degradation pathways in Parkinson's disease: curse or blessing. *Acta Neuropathol* **124**: 153–72.

El-Horany HE, El-Latif RN, ElBatsh MM, Emam MN. (2016). Ameliorative Effect of Quercetin on Neurochemical and Behavioral Deficits in Rotenone Rat Model of Parkinson's Disease: Modulating Autophagy (Quercetin on Experimental Parkinson's Disease). *J Biochem Mol Toxicol* **30**: 360–9.

Exner N, Lutz AK, Haass C, Winklhofer KF. (2012). Mitochondrial dysfunction in Parkinson's disease: molecular mechanisms and pathophysiological consequences. *EMBO J* **31**: 3038–62.

Fahn S, Sulzer D. (2014). Neurodegeneration and neuroprotection in Parkinson disease. *NeuroRx* **1**: 139–54.

Federico A, Cardaioli E, Da Pozzo P, Formichi P, Gallus GN, Radi E. (2012). Mitochondria, oxidative stress and neurodegeneration. *J Neurol Sci* **322**: 254–62.

Galehdar Z, Swan P, Fuerth B, Callaghan SM, Park DS, Cregan SP. (2010). Neuronal apoptosis induced by endoplasmic reticulum stress is regulated by ATF4-CHOP-mediated induction of the Bcl-2 homology 3-only member PUMA. *J Neurosci* **30**: 16938–48.

Halperin L, Jung J, Michalak M. (2014). The many functions of the endoplasmic reticulum chaperones and folding enzymes. *IUBMB Life* **66**: 318–26.

Hauser DN, Hastings TG. (2013). Mitochondrial dysfunction and oxidative stress in Parkinson's disease and monogenic parkinsonism. *Neurobiol Dis* **51**: 35–42.

Hoozemans JJ, Scheper W. (2012). Endoplasmic reticulum: the unfolded protein response is tangled in neurodegeneration. *Int J Biochem Cell Biol* **44**: 1295–8.

Hosoi T, Ozawa K. (2009). Endoplasmic reticulum stress in disease: mechanisms and therapeutic opportunities. *Clin Sci (Lond)* **118**: 19–29.

Hu LW, Yen JH, Shen YT, Wu KY, Wu MJ. (2014). Luteolin modulates 6-hydroxydopamine-induced transcriptional changes of stress response pathways in PC12 cells. *PLoS One* **9**: e97880.

Jha SK, Jha NK, Kumar D, Ambasta RK, Kumar P. (2017). Linking mitochondrial dysfunction, metabolic syndrome and stress signaling in Neurodegeneration. *Biochim Biophys Acta* **1863**: 1132–1146.

Joshi DC, Bakowska JC. (2011). Determination of mitochondrial membrane potential and reactive oxygen species in live rat cortical neurons. *J Vis Exp* **51**: pii. 2704.

Khan MM, Raza SS, Javed H, Ahmad A, Khan A, Islam F, Safhi MM, Islam F. (2012). Rutin protects dopaminergic neurons from oxidative stress in an animal model of Parkinson's disease. *Neurotox Res* **22**: 1–15.

Kim-Han JS, O'Malley KL. (2007). Cell stress induced by the parkinsonian mimetic, 6-hydroxydopamine, is concurrent with oxidation of the chaperone, ERp57, and aggresome formation. *Antioxid Redox Signal* **9**: 2255–64.

Kim Y, Li E, Park S. (2012). Insulin-like growth factor-1 inhibits 6-hydroxydopamine-mediated endoplasmic reticulum stress-induced apoptosis via regulation of heme oxygenase-1 and Nrf2 expression in PC12 cells. *Int J Neurosci* **122**: 641–9.

Kondratyev M, Avezov E, Shenkman M, Groisman B, Lederkremer GZ. (2007). PERK-dependent compartmentalization of ERAD and unfolded protein response machineries during ER stress. *Exp Cell Res* **313**: 3395–407.

Kulich SM, Horbinski C, Patel M, Chu CT. (2007). 6-Hydroxydopamine induces mitochondrial ERK activation. *Free Radic Biol Med* **43**: 372–83.

Lee AH, Iwakoshi NN, Glimcher LH. (2003). XBP-1 regulates a subset of endoplasmic reticulum resident chaperone genes in the unfolded protein response. *Mol Cell Biol* **23**: 7448–59.

Leitman J, Ron E, Ogen-Shtern N, Lederkremer GZ. (2013). Compartmentalization of endoplasmic reticulum quality control and ER-associated degradation factors. *DNA Cell Biol* **32**: 2–7.

Li B, Xiao L, Wang ZY, Zheng PS. (2014). Knockdown of STIM1 inhibits 6-hydroxydopamine-induced oxidative stress through attenuating calcium-dependent ER stress and mitochondrial dysfunction in undifferentiated PC12 cells. *Free Radic Res* **48**: 758–68.

Li Y, Li J, Li S, Li Y, Wang X, Liu B, Fu Q, Ma S. (2015). Curcumin attenuates glutamate neurotoxicity in the hippocampus by suppression of ER stress-associated TXNIP/NLRP3 inflammasome activation in a manner dependent on AMPK. *Toxicol Appl Pharmacol* **286**: 53–63.

Magalingam KB, Radhakrishnan A, Haleagrahara N. (2016). Protective effects of quercetin glycosides, rutin, and isoquercetrin against 6-hydroxydopamine (6-OHDA)-induced neurotoxicity in rat pheochromocytoma (PC-12) cells. *Int J Immunopathol Pharmacol* **29**: 30–9.

Martín-Aragón S, Jiménez-Aliaga KL, Benedí J, Bermejo-Bescós P. (2016). Neurohormetic responses of quercetin and rutin in a cell line over-expressing the amyloid precursor protein (APPswe cells). *Phytomedicine* **23**(12): 1285–1294.

Martorell M, Forman K, Castro N, Capó X, Tejada S, Sureda A. (2016). Potential Therapeutic Effects of Oleuropein Aglycone in Alzheimer's Disease. *Curr Pharm Biotechnol* **17**: 994–1001.

Mattson MP, Cheng A. (2006). Neurohormetic phytochemicals: Low-dose toxins that induce adaptive neuronal stress responses. *Trends Neurosci* **29** (11): 632–9.

Meng H, Li C, Feng L, Cheng B, Wu F, Wang X, Li Z, Liu S. (2007). Effects of Ginkgolide B on 6-OHDA-induced apoptosis and calcium over load in cultured PC12. *Int J Dev Neurosci* **25**: 509–14.

Mercado G, Castillo V, Vidal R, Hetz C. (2015). ER proteostasis disturbances in Parkinson's disease: novel insights. *Front Aging Neurosci* **7**: 39.

Mercado G, Valdés P, Hetz C. (2013). An ERcentric view of Parkinson's disease. *Trends Mol Med* **19**: 165–75.

Muralidharan S, Mandrekar P. (2013). Cellular stress response and innate immune signaling: integrating pathways in host defense and inflammation. *J Leukoc Biol* **94**: 1167–84.

Murugaiyah V, Mattson MP. (2015). Neurohormetic phytochemicals: An evolutionary-bioenergetic perspective. *Neurochem Int* **89**: 271–80.

Ogen-Shtern N, Ben David T, Lederkremer GZ. (2016). Protein aggregation and ER stress. *Brain Res* **1648**: 658–666.

Pantano D, Luccarini I, Nardiello P, Servili M, Stefani M, Casamenti F. (2017). Oleuropein aglycone and polyphenols from olive mill wastewater ameliorate cognitive deficits and neuropathology. *Br J Clin Pharmacol* **83**: 54–62.

Pasban-Aliabadi H, Esmaeili-Mahani S, Sheibani V, Abbasnejad M, Mehdizadeh A, Yaghoobi MM. (2013). Inhibition of 6-hydroxydopamine-induced PC12 cell apoptosis by olive (Olea europaea L.) leaf extract is performed by its main component oleuropein. *Rejuvenation Res* **16**: 134–42.

Penke B, Bogár F, Fülöp L. (2016). Protein Folding and Misfolding, Endoplasmic Reticulum Stress in Neurodegenerative Diseases: in Trace of Novel Drug Targets. *Curr Protein Pept Sci* **17**: 169–82.

Perri ER, Thomas CJ, Parakh S, Spencer DM, Atkin JD. (2016). The Unfolded Protein Response and the Role of Protein Disulfide Isomerase in Neurodegeneration. *Front Cell Dev Biol* **3**: 80.

Pourkhodadad S, Alirezaei M, Moghaddasi M, Ahmadvand H, Karami M, Delfan B, Khanipour Z. (2016). Neuroprotective effects of oleuropein against cognitive dysfunction induced by colchicine in hippocampal CA1 area in rats. *J Physiol Sci* **66**: 397–405.

Rieger AM, Nelson KL, Konowalchuk JD, Barreda DR. (2011). Modified annexin V/propidium iodide apoptosis assay for accurate assessment of cell death. *J Vis Exp* **50**: 2597.

Rigacci S, Stefani M. (2016). Nutraceutical Properties of Olive Oil Polyphenols. An Itinerary from Cultured Cells through Animal Models to Humans. *Int J Mol Sci* **17**: E843.

Rodríguez-Morató J, Xicota L, Fitó M, Farré M, Dierssen M, de la Torre R. (2015). Potential role of olive oil phenolic compounds in the prevention of neurodegenerative diseases. *Molecules* **20**: 4655–80.

Sarbishegi M, Mehraein F, Soleimani M. (2014). Antioxidant role of oleuropein on midbrain and dopaminergic neurons of substantia nigra in aged rats. *Iran Biomed J* **18**: 16–22.

Schroder M, Kaufman RJ. (2005). ER stress and the unfolded protein response. *Mutat Res* **569**: 29–63.

Sun X, Liu J, Crary JF, Malagelada C, Sulzer D, Greene LA, Levy OA. (2013). ATF4 protects against neuronal death in cellular Parkinson's disease models by maintaining levels of parkin. *J Neurosci* **33**: 2398–407.

Szegezdi E, Logue SE, Gorman AM, Samali A. (2006). Mediators of endoplasmic reticulum stress-induced apoptosis. *EMBO Rep* **7**: 880–5.

Taylor JM, Main BS, Crack PJ. (2013). Neuroinflammation and oxidative stress: co-conspirators in the pathology of Parkinson's disease. *Neurochem Int* **62**: 803–19.

Tsai YC, Weissman AM. (2010). The Unfolded Protein Response, Degradation from Endoplasmic Reticulum and Cancer. *Genes Cancer* **1**: 764–778.

Tsuru A, Imai Y, Saito M, Kohno K. (2016). Novel mechanism of enhancing IRE1α-XBP1 signalling via the PERK-ATF4 pathway. *Sci Rep* **6**: 24217.

Valdés P, Mercado G, Vidal RL, Molina C, Parsons G, Court FA, Martinez A, Galleguillos D, Armentano D, Schneider BL, Hetz C. (2014). Control of dopaminergic neuron survival by the unfolded protein response transcription factor XBP1. *Proc Natl Acad Sci U S A* **111**: 6804–9.

Wang YH, Xuan ZH, Tian S, Du GH. (2015). Echinacoside Protects against 6-Hydroxydopamine-Induced Mitochondrial Dysfunction and Inflammatory Responses in PC12 Cells via Reducing ROS Production. Evid. Based Complement. *Alternat Med* **2015**: 189239.

Wu PS, Yen JH, Kou MC, Wu MJ. (2015). Luteolin and Apigenin Attenuate 4-Hydroxy-2-Nonenal-Mediated Cell Death through Modulation of UPR, Nrf2-ARE and MAPK Pathways in PC12 Cells. *PLoS One* **10**: e0130599.

Zeeshan HM, Lee GH, Kim HR, Chae HJ. (2016). Endoplasmic Reticulum Stress and Associated ROS. *Int J Mol Sci* **17**: 327.

Zhai X, Ding Y, Wang Q, Zhang H, Li F. (2016). Rutin Acid Ameliorates Neural Apoptosis Induced by Traumatic Brain Injury via Mitochondrial Pathways in Mice. *Neuroimmunomodulation* **23**: 179–187.

Zhang C, Li C, Chen S, Li Z, Jia X, Wang K, Bao J, Liang Y, Wang X, Chen M, Li P, Su H, Wan JB, Lee SMY, Liu K, He C. (2017). Berberine protects against 6-OHDA-induced neurotoxicity in PC12 cells and zebrafish through hormetic mechanisms involving PI3K/AKT/Bcl-2 and Nrf2/HO-1 pathways. *Redox Biol* **11**: 1–11.

Zhang C, Li C, Chen S, Li Z, Ma L, Jia X, Wang K, Bao J, Liang Y, Chen M, Li P, Su H, Lee SM, Liu K, Wan JB, He C. (2017). Hormetic effect of panaxatriol saponins confers neuroprotection in PC12 cells and zebrafish through PI3K/AKT/mTOR and AMPK/SIRT1/FOXO3 pathways. *Sci Rep* **7**: 41082.

Zuo L, Motherwell MS. (2013). The impact of reactive oxygen species and genetic mitochondrial mutations in Parkinson's disease. *Gene* **532**: 18–23.